Molecular Orientation and Morphology of Organized Molecular Films for Fluorinated Comb Copolymers

Atsuhiro Fujimori,[*1] *Satoshi Kobayashi,*[1] *Ryosuke Masuya,*[1] *Toru Masuko,*[1] *Eisuke Ito,*[2] *Masahiko Hara,*[2] *Kaname Kanai,*[3] *Yukio Ouchi,*[3] *Kazuhiko Seki,*[3,4] *Hiroo Nakahara*[5]

Summary: Surface morphology of monolayers related to solid-state structure for methacrylate comb copolymers having fluorocarbon and hydrocarbon side-chains was investigated by X-ray diffraction (XRD), differential scanning calorimetry (DSC), and atomic force microscopy (AFM). From the XRD profiles, two kinds of short spacing peaks were confirmed at 5.0 and 4.2 Å, which assigned the sub-cells for both side-chains. Furthermore, two kinds of endothermic peaks, which corresponded to melting peaks of the both side-chain crystals, appeared in the thermograms. From the AFM observation, it was found that there were hydrogenated domains at a few hundred nm diameter in their monolayers, whereas corresponding acrylate copolymer monolayers form the phase-separated structure at 10–30 nm order scales.

Keywords: comb copolymer; fluorocarbon; molecular arrangement; organized molecular films; phase separation

Introduction

Fluorinated compounds including fluoropolymers have attracted wide interested in the fundamental material sciences and applied technologies for the past fifty years,[1,2] since the fluorinated surface is effective on the tribological behavior due to the low energy surface[3] and negative surface potentials[4] in addition to their excellent thermal stability and chemical resistance. In the view of industrial field, fluoropolymers also have been used on several fields as oil-resistant rubbers for using at high temperature, and fluorine manufactured products. The character of these polymers containing fluorocarbon chains has been based on the properties of fluorocarbon chain such as good rubbing-resistant, chemical-resistant and surface activity. For the last quarter of a century, fluorinated functional materials have been synthesized to compare with corresponding hydrocarbon derivatives.[5–10] Surfactants with fluorocarbons in solutions are known to exhibit different behaviors from those of the corresponding amphiphiles with hydrocarbons.[11] Fluorinated amphiphiles and polymerizable lipids were synthesized for formation of biomembrane models.[12–15] Recently, the polymers with fluorocarbon side-chains were reported for the practical utilization in the lubricant at low temperatures.[16] Molecular orientation of the partially fluorinated amphiphiles in the monolayers at the air/water interface and the wettability of those adsorbed films were examined early in comparison with those of the hydrocarbon derivatives.[4,17]

On the other hand, the surface patterning[18,19] is an important subject for

[1] Faculty of Engineering, Yamagata University Jonan 4-3-16, Yonezawa, Yamagata, 992-8510 Japan
Tel and Fax: +81-238-26-3073
E-mail: fujimori@ yz.yamagata-u.ac.jp
[2] Local Spatio-Temporal Function, Frontier Research System, The Institute of Physical and Chemical Reserch (RIKEN), Wako 351-0198 Japan
[3] Graduate School of Science, Nagoya Univ., Nagoya 464-8602, Japan
[4] Research Center for Material Science, Nagoya Univ., Nagoya 464-8602, Japan
[5] Facuty of Science, Saitama University, Saitama 338-8570, Japan

development of new molecular devices as lithography. It is well known that characteristic phase separation occurs in the mixed materials containing fluorocarbons and hydrocarbons because of the lack of miscibility.[5,20] Since H. J. Güntherodt, et al. reported studies on mixed monolayer system containing fluorinated compounds estimated by friction force microscopy,[6] several mixed systems of fluorinated and hydrogenated compounds in the three-dimensional composites and two-dimensional organized molecular films were widely examined by many investigators. However, the surface patterning at the nanometer length scale is impossible in this phase-separated system still now, because the hydrogenated domains in the phase-separated structure are generally size of a few μm.[20–23] This phenomenon may be caused by the expand phase (sea region) formed by unoriented fluorinated compounds. The two-dimensional micro phase separation itself in the mixed monolayer is caused by line tension of domains or by two-dimensional spinodal decomposition. However, whichever process may occur, the 'sea region' is generally an expanded phase. It seems that existence of commonly oriented island and sea phase is a key to the realization of nano-patterning using mixed system of fluorocarbons and hydrocarbons. In order to solve this proposition, there are many possibilities of utilizing the micro phase separation in three-dimensional block copolymers. If phase separation of this type is used for the surface patterning at the nanometer length scale and can be controlled by changes in the monomer ratio on the co-polymerization, it is interesting in the scopes of not only basic science but also nano-technology.

Previously, the monolayers of the comb polymers with hydrocarbon side-chains such as poly(octadecyl acrylate) and poly (vinyl stearate), which were obtained by γ-ray irradiation to the corresponding monomers in solid states, were found to be effective on the retardation of water evaporation by the binary mixed monolayers of poly(vinyl esters of long-chains) with octadecanol or hexadecanol,[24] in which the microstructures of the mixed monolayers were observed by atomic force microscopy.[25] Recently, instead of the hydrocarbon chains, monomers of acrylates and methacrylates containing various fluorocarbon chains with different lengths and fluorine atoms at the ω-position were used on monolayers formation at the air/water interface.[26] Furthermore, the comb polymers containing various fluorocarbon side-chains with various lengths and fluorine atoms at the ω-position were obtained using post-polymerization of these corresponding monomers irradiation of ^{60}Co γ-ray at $-196\,^{\circ}C$ in liq. $-N_2$.[27,28] Stabilities of the monolayers and the multilayer formation of the fluorinated monomer amphiphiles with the vinyl groups were studied,[29] and the monolayer assemblies of the corresponding fluorinated comb polymers were also reported.[30] Early on this work, the solid-state structure and morphology of monolayer of newly synthesized fluorinated acrylate comb copolymers investigated by wide-angle X-ray diffraction (WAXD), and atomic force microscopy (AFM).[31]

In the present paper, the fine structure in the solid state of newly synthesized fluorinated methacrylate comb copolymers by wide-angle X-ray diffraction (WAXD). Furthermore, phase transition behavior of these comb copolymers was examined by differential scanning calorimeter (DSC) and temperature controlled WAXD measurements. In addition, these methacrylate comb copolymers are formed extremely condensed monolayers on the water surface. Their transferred films on mica are exhibited phase separated surface at $\mu m \sim$ sub-micron scales whereas previous reported corresponding acrylate monolayers form the patterned structure at 10–30 nm scales. Generally, since poly-acrylic and poly-methacrylic acids are amorphous and crystalline polymers, respectively, the reason of those difference of surface morphology is suggested influence of packing hindrance for fluorinated side-chain by arrangement of high crystallinity methacrylate main-chain.

Experimental

Materials

Fluorinated comb copolymers were obtained by copolymerization of octadecyl methacrylate (OMA) and 2-(perfluorodecyl)ethyl methacrylate ($FF_{10}EMA$) at several monomer ratios. Copolymerizations were carried out in a solution of $CHCl_3$ at 50 °C for 48 hours using 1 mol% azobisisobutyronitrile (AIBN) as initiator. The precipitated polymers were washed with acetone till they were free of monomers. The syndiotactic Poly-$FF_{10}EMA$ homopolymer were obtained only by 1 Mrad ^{60}Co γ-ray irradiated post-polymerization according to the same procedure given in the previous work.[28] Comb copolymer compositions were determined by ^1H NMR spectroscopy. The tacticity of fluorinated homopolymer was obtained to be almost syndiotactic (Diad; 57.4%) by ^1H NMR analysis according to the reference.[32] The molecular weights of several copolymers with higher ratios of OMA units were estimated to be about $\overline{M}_w = 3.5 - 5.0 \times 10^4 (\overline{M}_w/\overline{M}_n \approx 2.2)$ on the basis of GPC measurement (see Table 1). The molecular weights of fluorinated homopolymer and copolymers with higher ratios of $FF_{10}EMA$ units were estimated to be above a thousand from the intrinsic viscosity of $[\eta] = 0.12 \sim 0.54$ for these trifluoroacetic acid solutions at 30 °C by applying the relation $[\eta] = KM^{\alpha}$, where $K = 0.24 \sim 0.25 \times 10^{-4}$, $\alpha = 0.75 \sim 0.78$ were assumed from results of viscosity-averaged molecular weight for poly-alkyl methacrylate.[33]

According to the results of ^1H NMR measurements, there is a great possibility of formation of the block-type random copolymer obtained by immiscible monomers. Probably, it cannot form many bonding points in the solution during the co-polymerization because immiscible monomers are hard to approach each other and form the bonding.

Structural Estimation of Bulk Copolymers

The thermal analyses were carried out by using a Seiko Instruments model DSC200 differential scanning calorimeter. The DSC measurements were performed with a scanning rate of 10.0 °C min^{-1} as standard. Sample mass of ca. 2.00 mg was used for all DSC measurements. As usual scanning of DSC measurements, heating and cooling cycle was repeated twice, in order to examine the difference of the peak position and the transition enthalpy between the 1st heating and the next.

The packing modes of the several copolymers in crystalline phase were examined by X-ray powder diffraction measurements using a Rigaku Rad-rA diffractometer with Cu*K*α radiation, which was equipped with a graphite monochrometer at 40 kV and at 200 mA. In the case of *in situ* elevating temperature measurements, the temperature range from 25 to 65 °C was adopted with reference to the results of DSC measurements.

Formation of Copolymer Monolayers on the Water Surface and Estimation of Molecular Arrangement in the Films

The monolayers of the fluorinated comb copolymer were spread from the chloroform/trifluoroacetic acid = 90/10 (v/v) mixed solutions (about 10^{-4} M) onto the distilled water (about 18 MΩ · cm). The surface pressure – area (π – A) isotherms of the polymers were measured on a Lauda film

Table 1.
GPC data of individual copolymers used in this study.

Copolymerization ratio ($FF_{10}EMA$:OMA)	$\overline{M}_n$ (/10^4)	$\overline{M}_w$ (/10^4)	$\overline{M}_w/\overline{M}_n$
0:1	3.52	8.88	2.52
1:8	5.94	13.14	2.21
1:5	5.04	11.24	2.23
1:3	4.14	7.92	1.91

balance at different temperatures. These fluorinated comb copolymers formed extremely condensed monolayers. These monolayers were deposited onto the solid substrates at r. t. by a surface lowering method[34] at 25 mNm^{-1} to obtain non-alternating Z-type film. For the outermost surface of Z-type films, the hydrophobic fluorocarbon side-chains were exposed to the air.

Surface morphologies of the transferred films were observed by a scanning probe microscope (Seiko Instrument, SPA300 with SPI-3800 probe station), using microfabricated rectangular Si_3N_4 cantilevers with integrated pyramidal tips with a constant force of 0.09 N/m). The long-spacing of the layered structures of the films on glass substrates were measured by an out-of plane X-ray diffractometer (Rigaku, Rad-rA, Cu$K\alpha$ radiation, 40 kV, 100 mA) equipped with a graphite monochromator. The in-plane spacings of the two-dimensional lattice of the films were determined by analysis of an X-ray diffractometer with different geometrical arrangements[35,36] (Bruker AXS, MXP-BX, Cu$K\alpha$ radiation, 40 kV, 40 mA, an article specially made to order) equipped with a parabolic graded multilayer mirror. The monomolecular level resolution of this in-plane XRD apparatus was realized by applying incident angle of the X-ray is 0.2°, and slow scanning at 0.05°/150 sec. (multilayers:0.05°/20 sec. scan).

Results and Discussion

Estimation of Fine Structures for Fluorinated Comb Copolymers

Figure 1 shows X-ray powder diffraction profiles of Poly-FF_{10}EMA, Poly-OMA and FF_{10}EMA:OMA = 1:2 fluorinated comb copolymer. From the WAXD profiles

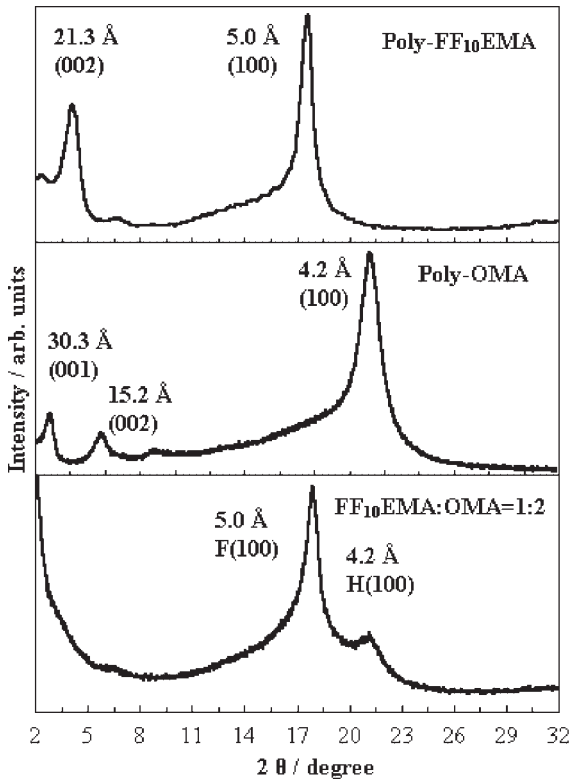

Figure 1.
XRD profiles of Poly-FF_{10}EMA, Poly-OMA, and FF_{10}EMA:OMA = 1:2 copolymer.

of each homopolymers, short spacing peaks based on the sub-cell of side-chains were confirmed at 4.2 and 5.0 Å. According to the Platé's review, these peaks correspond to (100) reflection.[37] In the case of copolymers, two kinds of short spacing peaks of side-chains were commonly confirmed at 4.2 and 5.0 Å. In the present work, these peaks were defined as H(100) and F(100) reflections, because these peaks were based on the structure in the different region of fluorinated copolymer crystal. In other words, since these values agree well with the in-plane lattice spacing of sub-cells for the homopolymers, it means that fluorinated and hydrogenated side-chains are separately packed in the phase-separated domains.

In the small angle region, the long spacing peaks are positioned at about 21.3 or 30.3 and 15.2 Å in the profiles of Poly-FF_{10}EMA and Poly-OMA. These polymers form the layer structure along the direction of c-axis. According to the previous work, it seems that this long spacing peak in the profile of Poly-FF_{10}EMA were defined at (002) reflection,[30] because Poly-FF_{10}EMA form the double layer structure, and also because the calculated length of fluorocarbon side-chain are estimated about 21 Å. The *d*-spacing from (001) reflection peak of Poly-OMA was estimated at 30.3 Å. This value is smaller than double layer structure of Poly-OMA, which is estimated the length along the c-axis at about 25 Å. According to the previous reports, the reason of smaller c-axis length is formation of interdigitated structure for Poly-OMA layers.[38,39] While, it was supported that FF_{10}EMA:OMA = 1:2 copolymer could not form the layer structure on this side-chain ratios.

Figure 2 shows WAXD profiles of fluorinated comb copolymers with several side-chain ratios. From these profiles, interesting systematic changes were confirmed in both long and short spacing region, which depended on the side-chain ratios. With an increase of OMA ratio, the intensity of (002) and F(100) reflection gradually decreased, and H(100) reflection appeared and grew from FF_{10}EMA:OMA = 1:1 copolymer to Poly-OMA. These XRD profiles indicate the possibility of structural control of side-chain crystals and its crystallinity that is reflected in peak width. This result will be very important information on the size and on the control of the dispersion degree for each domain related to surface pattering on the occasion of formation for the organized molecular films as following discussion.

From the results of WAXD measurements, the models of molecular arrangement and packing of fluorinated comb copolymers are shown in Fig. 3. The lengths of c-axis of Poly-OMA and Poly-FF_{10}EMA are 30.3 and 42.0 Å, respectively. Both homopolymers form the layer structure, especially in the case of Poly-OMA form the interdigitated structure. In addition, it seems that the side-chains of both hydro- and fluorocarbons of all copolymers synthesized in this work are packed two-dimensionally in hexagonal sub-cells, like Fig. 3(b).

Thermal Behavior of Comb Copolymers with Fluoro- and Hydrocarbon Side-Chains

Figure 4 shows typical DSC thermogram of FF_{10}EMA:OMA = 1:1 copolymer (scanning rate; 10 °C min^{-1}). Two kinds of endothermic peaks can be seen in the heating process, and other exothermic peaks can be seen in the cooling process. This supports the existence of two kinds of side-chain crystals. These transition peaks show the melting and crystallization peaks of fluorinated and hydrogenated side-chain crystals exhibiting different melting temperatures. In comparison with general crystalline polymers, the melting peaks of Poly-OMA and Poly-FF_{10}EMA in the DSC thermograms are sharp and they appear in relatively low temperature regions (about 35 °C and 130 °C, respectively) because side-chain crystal packed monomer-like (or general long-chain compounds with low molecular weight) structure forms. Therefore, the transition peaks at higher and lower temperature region should

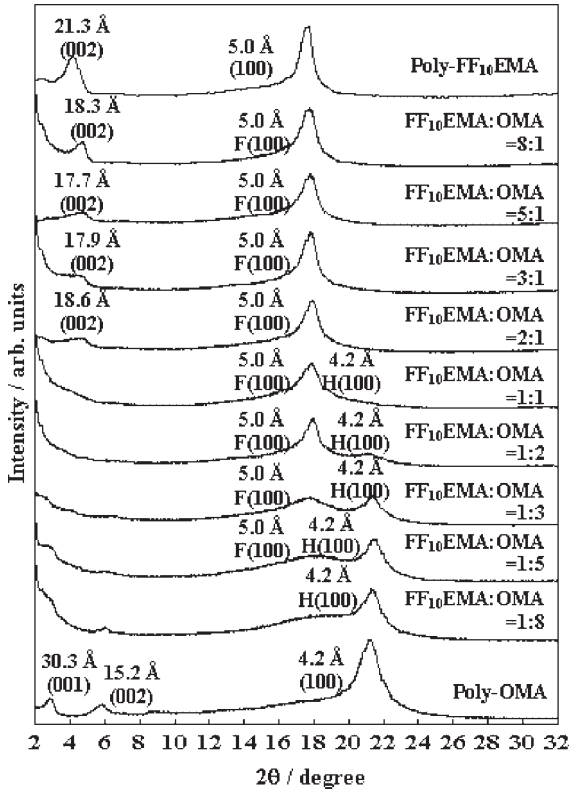

Figure 2.
XRD profiles of fluorinated comb copolymers with several ratios.

correspond to those of fluorocarbon and hydrocarbon side-chain crystals, respectively.

Figure 5 displays 2nd-heating processes of DSC thermograms for each homopolymer and copolymers. On going from Poly-OMA to FF_{10}EMA:OMA = 1:1 copolymer, the peak positions in the low temperature side hardly move with a variation in FF_{10}EMA ratios. In the case of peaks in the high temperature side, those don't shifted with OMA ratios except the one of FF_{10}EMA:OMA = 1:1 and 1:2 copolymers, although these peaks sprit within the region of 90–130 °C, which mean the existence of different thickness of 'lamellae' (in this case, this term is able to exchange to the 'layers'). It is supposed that the melting peak shift to the low temperature side of fluorinated side-chain crystal of FF_{10}EMA:OMA = 1:1 and 1:2 copolymers means a subtle miscibility of both side-chain crystals on these composition. Although copolymers with the exception of 1:1 and 1:2 copolymer also show the two kinds of peaks at much faster scanning rates ($20 \sim 100$ °C min^{-1}), this tendency is essentially invariable.

Figure 6 and 7 exhibit the plots of onset temperature for melting and fusion enthalpy *vs.* FF_{10}EMA composition, which can be confirmed at scanning rate 10 °C min^{-1}. The almost constant value of both melting temperatures is supposed completely phase separated structure between hydrogenated and fluorinated region in these copolymers. While, decrease of melting temperature for the fluorinated side-chain crystal of FF_{10}EMA:OMA = 1:1 and 1:2 copolymers (FF_{10}EMA ratios; 50 and 65%) are interpreted the existence of affinity between fluorinated and hydroge-

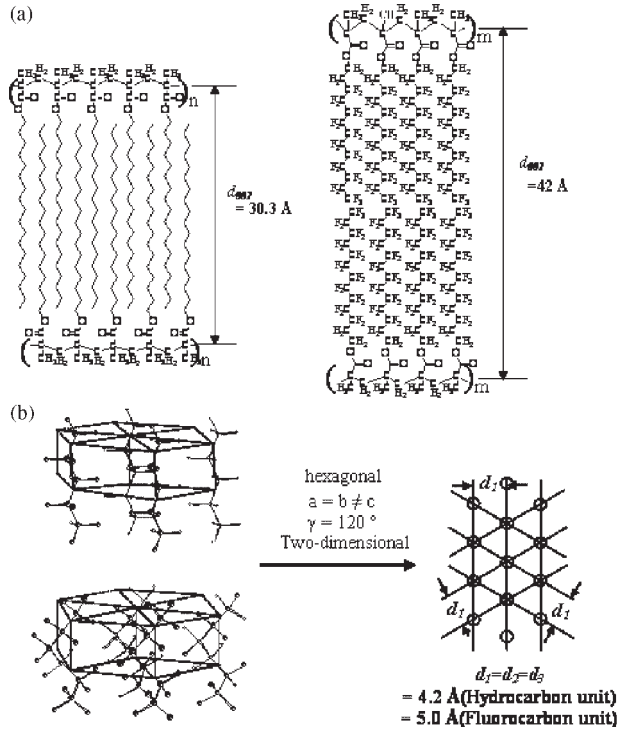

Figure 3.
Schematic illustration of layer structure for the (a) Poly-OMA and Poly- $FF_{10}EMA$ and (b) Sub-cell structure and two-dimensional lattice of hydrogenated and fluorinated side-chain crystals.

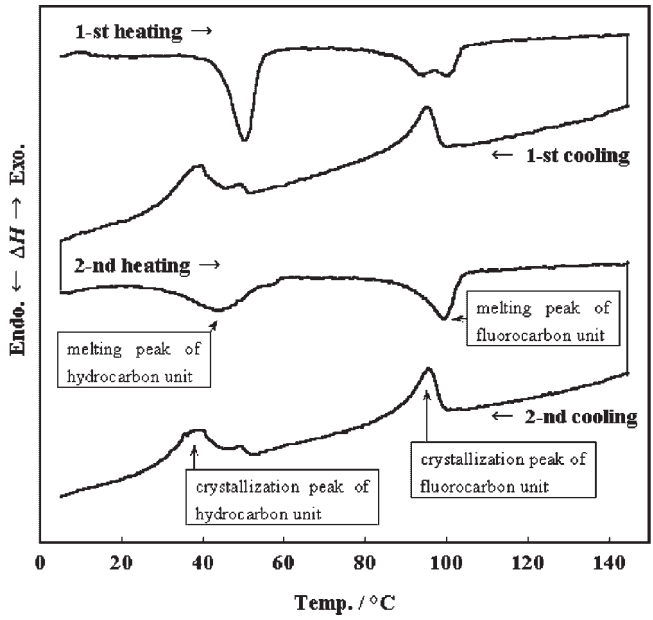

Figure 4.
DSC thermogram of $FF_{10}EMA$:OMA=1:1 copolymer (scanning rate; 10 °Cmin^{-1}).

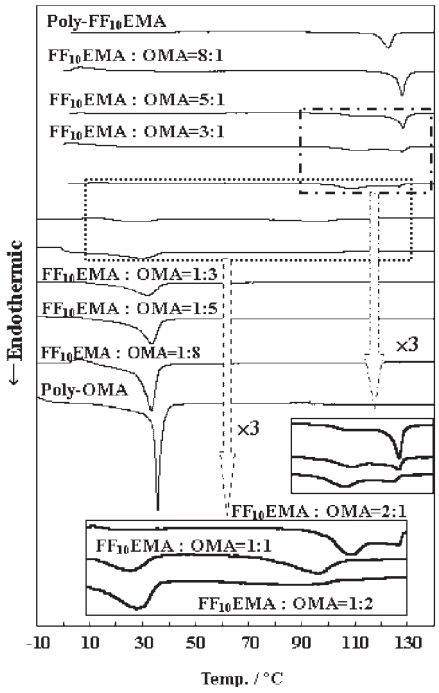

Figure 5.
DSC thermograms of fluorinated comb copolymers with several ratios (2nd-heating, scanning rate; 10 °Cmin^{-1}).

nated domains. That is to say, it is guessed that hydrogenated domains invade the fluorinated region.

In Fig. 7, the systematic changes are confirmed on the relationships between fusion enthalpy *vs.* $FF_{10}EMA$ compositions. Both fusion enthalpies are clearly depended on the composition, respectively.

In order to get accurate supported data of the existence of two kinds of side-chain crystals and to draw an inference from the thermal behavior, the temperature controlled X-ray diffraction was carried out. These profiles of $FF_{10}EMA:OMA = 1:2$ copolymer on elevating and cooling processes are shown in Fig. 8. Temperature controlled XRD measurements were carried out at three stages. At first, it was measured at room temperature. With the elevating temperature till 65 °C, the H(100) reflection disappears together with the melting of hydrogenated side-chain crystal. This result supports the DSC results and our speculation. When this sample is cooled down to 25 °C again, the H(100) reflection appears because of crystallization of the hydrogenated side-chain. Hence, it is concluded that reversible phase transition occurs in this copolymer system.

Molecular Arrangement of Organized Molecular Films for Fluorinated Comb Copolymers

On these experimental results, we try to make use of these fluorinated comb copolymers as the material for formation of monolayers on the water surface. From the surface pressure – area (π-A) isotherms,

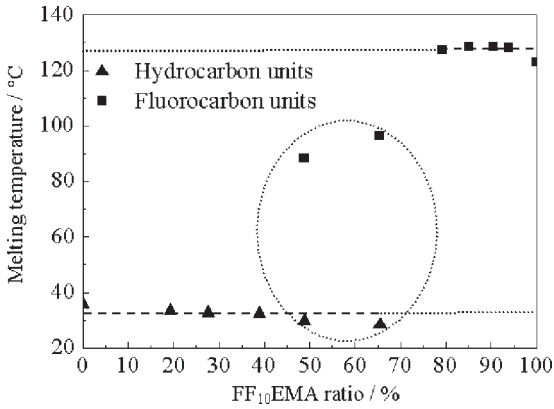

Figure 6.
Plots of peak top and on set temperature vs. $FF_{10}EMA$ ratio in fluorinated comb copolymers estimated from DSC thermograms.

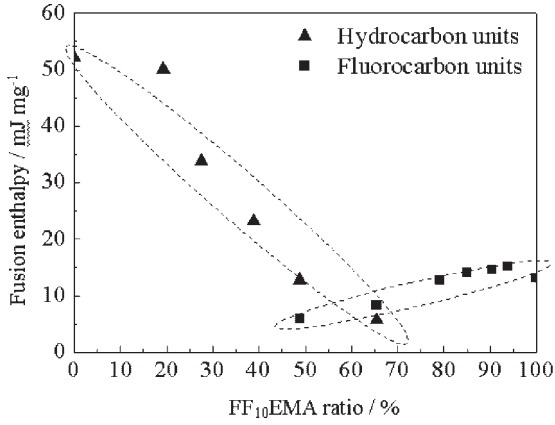

Figure 7.
Plots of fusion enthalpy of side-chain crystals vs. $FF_{10}EMA$ ratio in fluorinated comb copolymers estimated from DSC thermograms.

these phase-separated fluorinated comb copolymers formed extremely stable condensed monolayers at the air/water interface and it was possible to transfer these monolayers on solid substrates.[40] Figure 9 shows the in-plane X-ray diffraction profiles of several transferred films (20 layers) of $FF_{10}EMA$:OMA copolymers and each homopolymers. These profiles indicate the packing mode in the organized molecular films of these copolymer system analogeus to the bulk state. Poly-$FF_{10}EMA$ multilayers (25 mNm^{-1}, 5 °C) transferred by horizontal lifting method[41] formed two-dimensional orthorhombic system which exhibit two kinds of short spacing. (This result was well-correspondence to the previous reports.[30,36]) In the case of Poly-OMA Langmuir-Blodgett (LB) film[42] (25 mNm^{-1}, r. t.), two-dimensional lattice form the hexagonal packing. Further, it is found that $FF_{10}EMA$:OMA = 1:1 and 1:2 copolymer LB films exhibited only one short spacing which mean formation of hydrogenated hexagonal sub-cell. That is to say, in the organized molecular films,

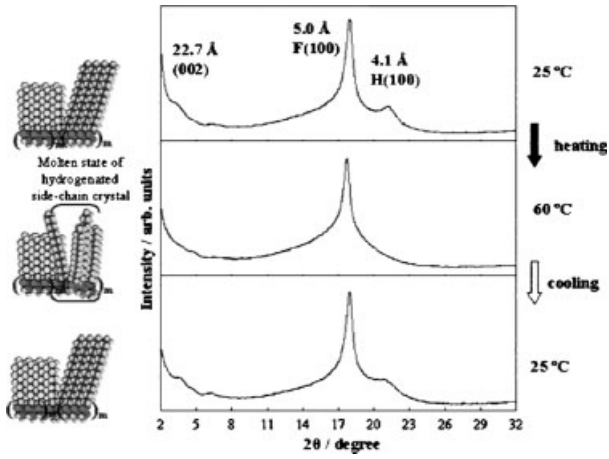

Figure 8.
Temperature controlled XRD profiles of $FF_{10}EMA$:OMA = 1:2 copolymer.

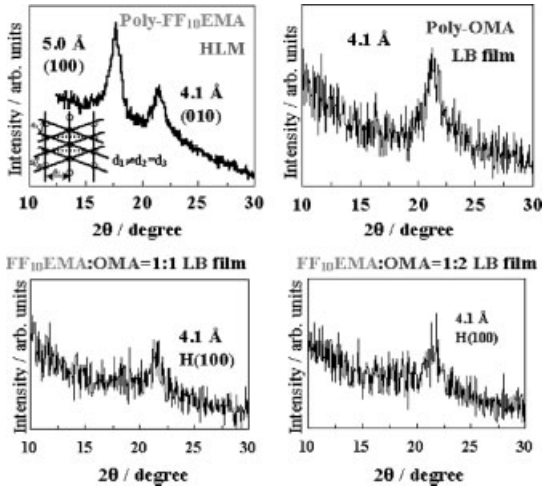

Figure 9.
In-plane XRD profiles of multilayers of Poly-$FF_{10}EMA$, OMA, $FF_{10}EMA$:OMA copolymers (20 layers, 25 mNm^{-1}, r. t.).

fluorinated region is corresponding to the expand phase, and hydrogenated region is condensed phase with highly order molecular orientation. Early on this work, the molecular orientation and surface morphology of monolayer and LB multilayers for corresponding acrylate comb polymer studied on in-plane XRD, AFM, and so on.[31,43] In the acrylate system (co-polymerization of octadecyl acrylate (OA) and 2-(perfluorodecyl)ethyl acrylate ($FF_{10}EA$) system), both oriented side-chain crystals in the copolymer film was formed, and miniaturized domains at 10–30 nm scales were confirmed by AFM. From the results of this previous work, we concluded the relationships between molecular orientation and formation of size-controlled domain in the 'sea'-'island' type phase-separated surface morphology. Hence, in the present work, we also examine the morphology of the monolayers related to the molecular arrangement, after that.

Surface Morphology of Monolayers on Solid for Fluorinated Comb Copolymers

Figure 10 shows AFM images of Z-type monolayers for $FF_{10}EMA$:OMA and previous reported $FF_{10}EA$:OA copolymer with various copolymerization ratios on mica at room temperature. In the case of $FF_{10}EMA$:OMA = 1:1 copolymer monolayer, circular domains made form the hydrogenated side-chain crystal at about 200–250 nm diameter and fluorinated 'sea' region were confirmed. While, in $FF_{10}EA$:OA = 1:1 copolymer monolayer, apparently homogeneous flat surface can be seen at 500×500 nm^2 scales. However, from the results of observation at the scale 100×100 nm^2 scales (two-dimensional image), nanometer order phase separated structure was confirmed. In addition, molecular resolution images of higher hill and around sea region commonly indicated dense packed regular structure of side-chain parts in comb copolymers. In the cross section of the surface in molecular resolution images along the dashed line of copolymer system, the distance between fluorocarbon side-chains in the 'sea' region was estimated the range from 4.9 to 5.4 Å, which well-corresponded to the value of the two-dimensional short spacing of this comb polymer measured by WAXD in the bulk state,[31,43] while the distance between hydrocarbons in the 'island' region exhibited the range from 3.9 to 4.3 Å. In both images of fluorocarbon and hydrocarbon

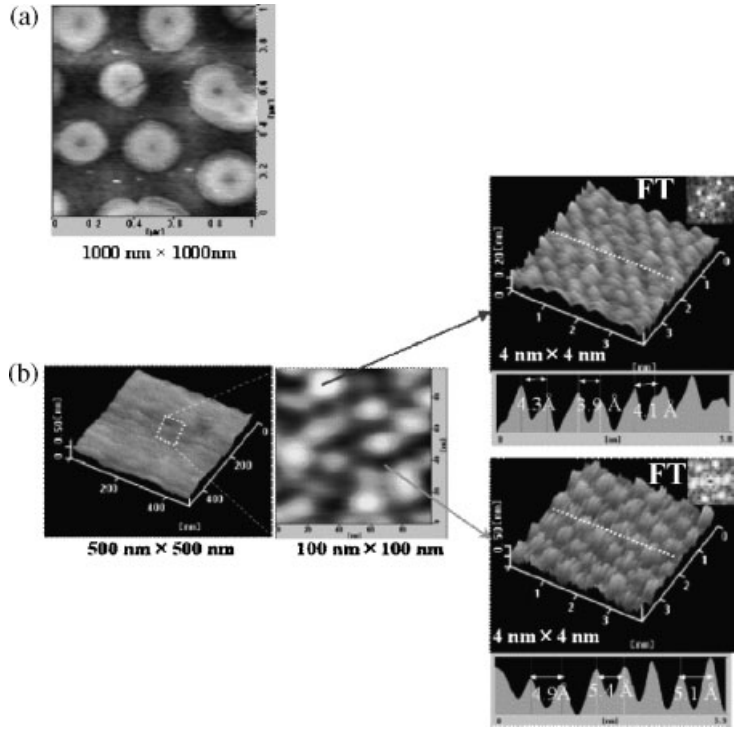

Figure 10.
AFM images of several Z-type monolayer on the mica substrate (25 mNm^{-1}, r. t.), (a) $FF_{10}EMA:OMA=1:1$ copolymer monolayer (1 $\mu m \times 1$ μm), (b) $FF_{10}EA:OA = 1:1$ copolymer monolayer at several magnification (500 nm × 500 nm, 100 nm × 100 nm, and 4 nm × 4 nm).

region, two-dimensional Fourier transformations (FT) were also shown in the insert figure. Both FT images exhibited the quasi-hexagon spot which was considered the formation of hexagonal systems on two-dimensional packing of side-chains.

Figure 11 show the AFM images of monolayers for comb copolymers in

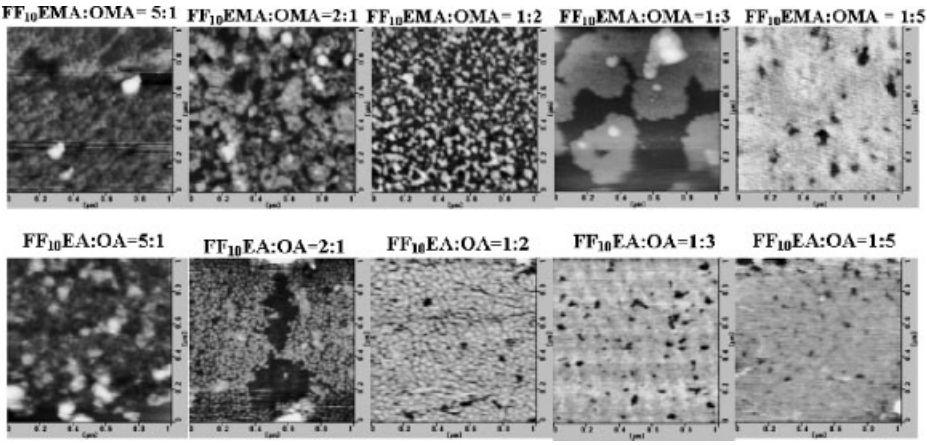

Figure 11.
AFM images of fluorinated comb copolymers with several ratios of Z-type monolayer on the mica substrate.

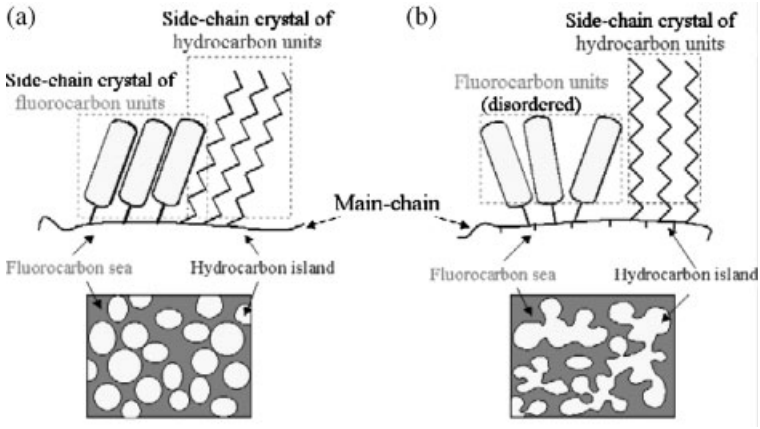

Figure 12.
Schematic illustration of molecular arrangement and surface morphology of fluorinated acrylate(a) and methacrylate(b) copolymer films.

methacrylic and acrylic system with several compositions at the $1 \times 1\ \mu m^2$ scales. With the increasing of hydrogenated side-chain ratio, the film surface is gradually covered by hydrogenated island, and fluorinated sea region decrease in the both systems. In the case of increasing of fluorinated side-chain ratio, the shape and alignment of hydrogenated domains gradually disordered. However, as the overview of formation of surface morphology on this acrylic system, it was possible to control construction of the phase separated structure at nonometer size by method of organized molecular films and copolymerization ratio of fluorinated comb copolymers. While, in the case of methacrylic system, it was confirmed obvious different tendency to the acrylic monolayer. The hydrogenated domain size of these methacrylic monolsyers are corresponded to the sub-micrometer scale. It is supposed that this difference closely relate the orientation regularity of fluorinated side-chain crystal. The result of morphological estimation is summarized in Fig. 12. Generally, since poly-acrylic acid and poly-methacrylic acid are amorphous and crystalline polymer, respectively, the reason of those difference of surface morphology is suggested influence of packing hindrance for fluorinated side-chain by arrangement of high crystallinity methacrylate main-chain. In conclusion, it is supposed to realize the nano-patterning at a few ten nanometer size on fluorocarbons and hydrocarbons system by existing commonly oriented island and sea phase. In other words, formation of sub-micron order phase separated surface structure on this type polymer monolayers is controlled by co-existence of expand fluorinated 'sea' phase and condensed hydrogenated 'island' phase. That is to say, it is possible to control patterned surface formed by methods of organized molecular films and co-polymerization of immiscible monomers. We think these results realized by assimilation of 'bottom-up' and 'top-down' nano-technologies.

Conclusions

The fine structure in the solid state and phase transition behavior of fluorinated methacrylate comb copolymers has been estimated by WAXD, DSC, and temperature controlled WAXD. From the results of these measurements, it is found that fluorinated and hydrogenated side-chain crystals of these comb copolymers were independently packed, and formed hexagonal sub-cell in the two-dimensional lattice. And further, it was indicated that

the phase transition also independently occurred at different temperature region between fluorocarbon and hydrocarbon side-chain crystals on the heating process of DSC measurement. From the results of AFM observation, it was found that there were hydrogenated domains at sub-micron diameter scales in these phase separated surface structure of monolayers on solids, whereas corresponding acrylate copolymer monolayers form the surface pattering structure at 10–30 nm order scales. The reason of these results is suggested hindrance of packing for fluorinated side-chain by arrangement of high crystallinity methacrylate main-chain.

[1] J. Burdon, J. C. Tatlow, in "*Advances in Fluorine Chemistry*", Vol. 1, M. Stacey, J. C. Tatlow, A. G. Sharp, Eds., Academic Press, New York, **1960**, p. 129–165.
[2] "*Fluoropolymers 2*" in *Topics in Applied Chemistry*, G. Hougham, et al., Eds., Kluwer Acad./Plenum Pub., New York, **1999**.
[3] E. G. Shafrin, W. A. Zisman, *J. Phys. Chem.*, **1957**, *61*, 1046.
[4] H. W. Fox, *J. Phys. Chem.*, **1957**, *61*, 1058.
[5] R. M. Overney, E. Meyer, J. Frommer, H.-J. Güntherodt, *Langmuir*, **1994**, *10*, 1281.
[6] R. M. Overney, E. Meyer, J. Frommer, D. Brodbeck, R. Luthi, L. Höwald, L., H.-J. Güntherodt, H. Fujihira, H. Takano, Y. Gotoh, *Nature*, **1992**, *359*, 133.
[7] R. Elbert, T. Folda, H. Ringsdorf, *J. Am. Chem. Soc.*, **1984**, *106*, 7687.
[8] R. H. Tredgold and G. W. Smith, *Thin Solid Films*, **1983**, *99*, 215.
[9] J. Schneider, C. Erdelen, H. Ringsdorf, and H. Rabolt, *Macromolecules*, **1989**, *22*, 3475.
[10] H. Hoffmann, G. Platz, H. Rehage, K. Reizlein, W. Ulbricht, *Makromol. Chem.*, **1981**, *182*, 451.
[11] (a) N. Funasaki and S. Hada, *J. Phys. Chem.*, **1980**, *84*, 736, (b) ibid., **84** (1980) 1868.
[12] A. Laschewsky, H. Ringsdorf, and G. Schmidt, *Thin Solid Films*, **1985**, *134*, 153.
[13] Y. Shibasaki, H. Nakahara, K. Fukuda, *J. Polym. Sci., Part A, Polym. Chem.*, **1979**, *17*, 2387.
[14] Y. Shibasaki, K. Fukuda, *J. Polym. Sci., Part A, Polym. Chem.*, **1979**, *17*, 2947.
[15] K. Fukuda, Y. Shibasaki, H. Nakahara, *Thin Solid Films*, **1998**, *160*, 43.
[16] M. K. Bernett, W. A. Zisman, *J. Phys. Chem.*, **1963**, *67*, 1534.
[17] V. K. Gupta, N. L. Abbott, *Science*, **1997**, *6*, 276.
[18] A. Kumar, A. Biebuyck, G. M. Whitesides, *Langmuir*, **1994**, *10*, 1498.
[19] K. Suga, Y. Iwamoto, H. Shibata, N. Yamada, M. Fujihira, *Thin Solid Films*, **1998**, *327–329*, 837.
[20] T. Imae, T. Takashita, M. Kato, *Langmuir*, **2000**, *16*, 612.
[21] S. Ge, A. Takahara, T. Kajiyama, *Langmuir*, **1995**, *11*, 1341.
[22] M. Matsumoto, K. Tanaka, R. Azumi, Y. Kondo, N. Yoshino, *Chem. Lett.*, **2002**, 970.
[23] K. Yagi, M. Fujihira, *Appl. Surf. Sci.*, **2000**, *157*, 405.
[24] K. Fukuda, T. Kato, S. Machida, Y. Shimizu, *J., Colloid Interface Sci.*, **1972**, *68*, 82.
[25] S. Machida, H. Nakahara, I. Yoshikawa, Y. Shibasaki, K. Fukuda, *Thin Solid Films*, **1998**, *327/329*, 109.
[26] A. Fujimori, T. Araki, H. Nakahara, *Chem. Lett.*, **2000**, 898.
[27] Y. Shibasaki, H. Saitoh, and K. Chiba, *J. Therm. Anal.*, **1997**, *49*, 115.
[28] A. Fujimori, H. Saitoh, and Y. Shibasaki, *J. Thermal. Anal.*, **1999**, *57*, 631.
[29] A. Fujimori, T. Araki, H. Nakahara, *J. Colloid Interface Sci.*, **2002**, *247*(2), 351.
[30] A. Fujimori, Y. Shibasaki, T. Araki, H. Nakahara, *Macromol. Chem. Phys.*, **2004**, *205*, 843.
[31] R. Masuya, N. Ninomiya, A. Fujimori., H. Nakahara, T. Masuko, *J. Polym. Sci., Part B, Polym. Phys.*, **2006**, *44*, 416.
[32] K. Yamada, T. Nakano, Y. Okamoto, *Polym. J.*, **1998**, *30*, 641.
[33] J. G. Fee, W. S. Port, L. P. Witnauer, *J. Polym Sci.*, **1958**, *33* (1958) 95.
[34] H. E. Ries, *J. Colloid Sci.*, **1961**, *16*, 361.
[35] A. Fujimori, Y. Sugita, H. Nakahara, E. Ito, M. Hara, N. Mtsuie, K. Kanai, Y. Ouchi, K. Seki, *Chem. Phys. Lett.*, **2004**, *387*, 345.
[36] A. Fujimori, T. Araki, H. Nakahara, E. Ito, M. Hara, H. Ishii, Y. Ouchi, K. Seki, *Chem. Phys. Lett.*, **2001**, *349*, 6.
[37] N. A. Platé, V. P. Shibaev, *J. Polym. Sci., Macromol. Rev.*, **1974**, *8*, 117.
[38] H. W. Hsieh, B. Post, H. Morawetz, *J. Polym. Sci., Part B, Polym. Phys.*, **1976**, *14*, 1241.
[39] K. Inomata, Y. Sakamaki, T. Nose, S. Sasaki, S., *Polym. J.*, **1996**, *28*(11), 992.
[40] A. Fujimori, R. Masuya, K. Kumagai, T. Masuko, E. Ito, M. Hara, K. Kanai, Y. Ouchi, K. Seki, *Trans. Mater. Res. Soc. Jpn.* **2005**, *30*(1), 143.
[41] K. Fukuda, H. Nakahara, T. Kato, *T. J. Colloid Interface Sci.*, **1976**, *54*, 430.
[42] G. L. Gains, Jr., *Insoluble Monolayers at Liquid Gus Interface*, Wiley: New York, **1966**.
[43] A. Fujimori, R. Masuya, T. Masuko, E. Ito, M. Hara, K. Kanai, Y. Ouchi, K. Seki, H. Nakahara, *Polym. Adv. Tech.*, **2006**, *17*(7), in press.

